Received: 15 February 2024 | Accepted: 27 November 2024

DOI: 10.1111/2041-210X.14489

Methods in Ecology and Evolution

RESEARCH ARTICLE

An integrative framework to combine migratory connectivity and demographic data

Killian A. Gregory[1,2] | Charlotte Francesiaz[3] | Frédéric Jiguet[2] | Pierre-André Crochet[1] | Pierrick Bocher[4] | Heinz Düttmann[5] | Jaanus Elts[6] | Thomas Fartmann[7] | Stefan Garthe[8] | Steffen Kämpfer[7] | Helmut Kruckenberg[9] | Riho Marja[10] | Markus Piha[11,12] | Philipp Schwemmer[8] | Aurélien Besnard[13]

[1]CEFE, University of Montpellier, CNRS, EPHE, IRD, Montpellier, France; [2]CESCO, MNHN-CNRS-Sorbonne Université, Paris, France; [3]OFB, DRAS, Juvignac, France; [4]Littoral Environnement et Sociétés Laboratory (LIENSs) La Rochelle University—CNRS, La Rochelle, France; [5]Niedersächsisches Ministerium für Umwelt, Energie und Klimaschutz, Hannover, Germany; [6]BirdLife Estonia, Tartu, Estonia; [7]Department of Biodiversity and Landscape Ecology, University of Osnabrück, Osnabrück, Germany; [8]Research and Technology Centre (FTZ), University of Kiel, Büsum, Germany; [9]Institute for Wetlands and Waterbird Research e.V., Verden, Germany; [10]'Lendület' Landscape and Conservation Ecology, Institute of Ecology and Botany, HUN-REN Centre for Ecological Research, Vácrátót, Hungary; [11]Natural Resources Institute Finland, Helsinki, Finland; [12]Finnish Museum of Natural History, University of Helsinki, Helsinki, Finland and [13]CEFE, Univ Montpellier, CNRS, EPHE-PSL University, IRD, Montpellier, France

Correspondence
Killian A. Gregory
Email: killian.gregory@cefe.cnrs.fr

Handling Editor: David Soto

Abstract

1. Migratory species experience various conditions and events throughout their annual cycle that influence their spatial and demographic dynamics. To understand these dynamics, it is essential to describe the origin and destination of individuals. Migratory connectivity, which is defined as the geographic linkage between populations across the annual cycle, is increasingly incorporated in population models to relate population trends to environmental variables at different stages of the cycle. However, such information on migratory movements is obtained independently from the study of population dynamics despite the interaction between both processes. Expanding on the growing use of integrated modelling approaches, we developed an integrated framework that allows the sharing of information between migratory connectivity and population data.
2. We first assembled an integrated migratory connectivity model and an integrated population model to join the analysis of GPS, live-reencounter, dead-recovery, capture–mark–recapture, and population count data within a unified framework. Based on simulated data, we assessed the ability of the resulting integrated connectivity and population model to produce unbiased and precise connectivity and demographic estimates. We then applied the same assessment to real data using the Eurasian Curlew (*Numenius arquata*) as a case study.
3. On simulated data, the integrated connectivity and population model estimated connectivity and survival parameters with no bias and similar precision to the

connectivity model alone. However, it outperformed the population model in estimating fecundity in the absence of explicit productivity data. When applied to the Eurasian Curlew, the integrated connectivity and population model produced overall similar migratory connectivity and more accurate demographic estimates than the connectivity model alone, consistent with previous studies. Additionally, the model was able to estimate fecundity, whereas the data were too sparse for the population model alone to disentangle juvenile survival and fecundity.

4. The sharing of information between migratory connectivity and population data improved the estimation of demographic parameters by the population model and improved connectivity parameter estimates when data were scarce. This flexible framework can be generalised to include diverse data on migration movements, population structure, individual heterogeneity or environmental variables, allowing further investigation of the interaction between migration patterns and population dynamics.

KEYWORDS
Bayesian framework, capture–mark–recapture, demography, GPS data, integrated modelling, migratory connectivity, population dynamics, ringing data

1 | INTRODUCTION

Migratory species engage in cyclical seasonal or transgenerational movements across countries and continents. Throughout their journey, they encounter diverse conditions, obstacles and threats that are likely to affect their fitness, either directly by increasing mortality rates (Sillett & Holmes, 2002) or through delayed effects carrying over to later in the migration cycle (Harrison et al., 2011; Marra et al., 1998). The population dynamics of migratory species thus depend on events occurring all around the migration cycle. Understanding the main factors that could impact the population dynamics of migratory species across their yearly cycles is essential to predict the adaptive responses of populations to selective pressures and to assess their vulnerability to local events or global changes (Finch et al., 2017; Webster et al., 2002). Yet investigating the consequences of events experienced by individuals at earlier migration stages, sometimes far from the monitored populations, that is seasonal interactions sensu Myers (1981) and Webster et al. (2002), requires a proper description of where individuals come from and where they go (Norris & Marra, 2007).

In species with large distributions, not all individuals are likely to migrate to the same area. Instead, they exhibit geographical variation in migration routes and non-breeding distributions. The links between populations or the sites they occupy throughout the migration cycle have been termed migratory connectivity (Webster et al., 2002). Accordingly, the study of migratory connectivity provides the information needed to understand the consequences of spatially localised events on the population network. Assessments of migratory connectivity range from qualitative descriptions of movement patterns to quantitative estimates of spatial correlations or transition probabilities between regions or populations (Gregory et al., 2023). Migratory connectivity has mainly been unravelled for birds, although some studies are beginning to provide insights into patterns for species with different migration cycles, such as marine mammals or insects (Dunn et al., 2019; Gao et al., 2020).

Various types of data that enable tracking individuals can inform about migratory connectivity. Most often, these data consist of locations for resightings or dead-recoveries of tagged individuals, trajectories collected using tracking technologies, or spatial assignments based on the comparison of isotopic or genetic signatures of samples with a reference map (Webster et al., 2002). Combining various datasets provides information at different geographic scales or for different subsets of the populations (Gregory et al., 2023). Migratory connectivity data are increasingly incorporated when addressing a range of ecological questions, deepening our understanding of migration patterns by studying their environmental and behavioural drivers (Norevik et al., 2020) or their consequences for population vulnerability (Jiguet et al., 2019).

The consequences of migratory connectivity on population dynamics are well-theorised (Runge et al., 2014), but there remains a lack of methodological tools to allow the joint study of migratory connectivity and variations in population sizes. Full-annual cycle (FAC) models, which take into account the effect of events all around the annual cycle on demographic trends (Hostetler et al., 2015), currently offer the most comprehensive framework for understanding the dynamics of migratory species. They allow, for instance, to correlate seasonal environmental variables with changes in abundance of migratory populations (Wilson et al., 2011) or to identify key features of migration networks on which to focus conservation efforts

(Hallworth et al., 2021; Taylor & Stutchbury, 2016). However, most FAC models rely on prior information on static migratory connectivity patterns to correlate seasonal effects with changes in population sizes (Hostetler et al., 2015; Marra et al., 2015), as migratory connectivity patterns and population dynamics are still studied independently. Current models therefore lack the ability to capture potential feedbacks between population dynamics and changes in migration patterns.

Data integration frameworks are rapidly spreading in ecology as they bear the potential of bringing together distinct fields of research (Zipkin et al., 2021). Data integration sensu stricto, also known as integrated modelling, refers to the joint analysis of multiple independent datasets within a single modelling framework. Compared to independent models, integrated models can extract more information from the data, improving the precision of estimates (Abadi, Gimenez, Arlettaz, & Schaub, 2010; Korner-Nievergelt et al., 2017). Additionally, they enable the estimation of parameters for which no explicit data are available, such as immigration rate or fecundity for integrated population models (Abadi, Gimenez, Ullrich, et al., 2010; Besbeas et al., 2002). The flexibility of data integration also allows the joint analysis of datasets with varying spatiotemporal resolutions and scales, combining their strengths and making up for discrepancies, provided significant differences in information content and sampling biases are accounted for (Saunders et al., 2019; Zipkin et al., 2021). Given its flexibility and properties, integrated modelling has the potential to bring together the analysis of migratory connectivity patterns and population dynamics, providing better understanding of their interplay (Hostetler et al., 2015).

In this study, we combine usual models from both fields of migratory connectivity and population dynamics to highlight a relationship between migratory connectivity and survival that allows their formal integration. Our aim was to provide a simple and reproducible example as a proof of concept to show that tools are available to bridge the gap between these two fields and to investigate how integrated modelling may benefit the estimation of migratory connectivity and demographic parameters. Combining data from breeding and non-breeding regions is likely to provide additional information on the demographic processes in each season, and their dependence on particular regions during the annual cycle. We first assembled an example of an integrated migratory connectivity and population model within an adaptable framework. We then assessed the performance of the resulting model on simulated data to quantify the gain in precision and reduction in bias of parameter estimates it provides compared to independent migratory connectivity or population models. Finally, we conducted a similar comparison using Eurasian Curlew data (*Numenius arquata*, hereafter curlew) as a case study to validate the applicability of the model to a real, unbalanced dataset. The perspectives of an integrated connectivity and population dynamics model are huge, as they open a new door to explicitly investigate the interaction between the demography of migratory populations and their movement patterns.

2 | MATERIALS AND METHODS

2.1 | Description of the models

The integrated connectivity and population model (ICPM) combines an integrated migratory connectivity model (ICM) and an integrated population model (IPM). These three integrated models combine model units for each independent dataset, which are described thereafter. Notations and parameters from the following sections are summarised in Table 1.

2.1.1 | Integrated migratory connectivity model (ICM)

The ICM aims to assess migratory connectivity between regions or populations. We chose to estimate quantitative connectivity parameters as transition probabilities $m_{g,k}$ between discrete breeding regions $g \in [1;G]$ and non-breeding regions $k \in [1;K]$, as this measure of migratory connectivity has direct relevance to population dynamics. A higher value of $m_{g,k}$ means that a higher proportion of the population moves from g to k, drawing a stronger connection between these two regions. The ICM combines simplified model units from the integrated models of Korner-Nievergelt et al. (2017), Procházka et al. (2017), Rushing et al. (2021) and Von Rönn et al. (2020) to jointly analyse ringing and tracking data. For each unit, individuals have been marked in breeding regions. Model units have been replicated for different age classes (individuals marked as adult or as juvenile) to account for age dependence in survival probabilities and some recapture probabilities (Table 1).

The first unit of the ICM fits live-reencounter data (LR) of individuals marked in breeding regions g and reencountered alive in non-breeding regions k. Adapted from Arnason-Schwarz multistate model by Korner-Nievergelt et al. (2017), it aims at estimating transition probabilities $m_{g,k}$ between certain states—here, presence in regions g and k. The probability of reencountering a bird of breeding region g in non-breeding region k alive is: $P_{LR}(g,k) = m_{g,k} \times p_k^{LR,age}$, where $p_k^{LR,age}$ is the probability of recapturing the individual given it is in region k. As the data are aggregated for all years, survival probabilities are confounded with reencounter probabilities $p_k^{LR,age}$, modelled as age-dependent to account for some of the variation in survival probabilities between juveniles and adults. Knowing the total number of marked individuals in each breeding population n_g^{Ringed} and the number of marked individuals never recaptured Q_g, the likelihood of the live-reencounter model takes the form:

$$\prod_{g=1}^{G} Multinom\left(LR_{g,1:K}, Q_g \middle| n_g^{Ringed}, m_{g,1:K}, p_{1:K}^{LR,age}\right). \quad (1)$$

The second unit of the ICM fits dead-recoveries (R) of individuals marked in breeding regions g whose remains were found in non-breeding regions k. Also adapted from Arnason-Schwartz

TABLE 1 Notations for data, parameters and indices used in the study.

Data	
$CMR_{t_C,t_R,g}$	*Capture–mark–recapture*: Three-dimensional m-array summarising the number of marked birds recaptured in the same region in year t_R after their last (re)capture in year t_C, over the monitoring period t^{CMR}, for each breeding population g
$LR_{g,k}$	*Live-Reencounter*: $G \times K$ matrix summarising the number of birds ringed in breeding region g and resighted alive in non-breeding region k
$R_{g,k\times t}$	*Dead bird recovery*: $G \times (K \times t)$ matrix summarising the number of birds ringed in breeding region g and recovered dead in non-breeding region k t years after ringing
$T_{g,k}$	*Tracking technologies*: $G \times K$ matrix summarising the number of birds tagged in breeding region g, tracked to non-breeding region k, and which data could be recovered
Q_g	Number of birds ringed in breeding region g that were never reencountered
n_g^{Ringed}, n_g^{Tagged}	Total number of birds ringed/tagged in breeding region g
$N_{g,t}$, $N_{g,t}^{obs}$, $N_{g,t}^{1}$, $N_{g,t}^{ad}$	*Population numbers*: True and observed number of breeding females (or pairs) N and N^{obs} of population g at time t, broken down into first-year (1) and adults (ad)
Parameters	
$m_{g,k}$	Migratory connectivity: transition probabilities from breeding region g to non-breeding region k
φ_k^{age}	Survival probabilities in non-breeding region k; age: for juveniles younger than 1 year (juv) and adults (ad)
Φ_g^{age}	Annual survival probabilities for birds of breeding region g; age: for juveniles younger than 1 year (juv) and adults (ad)
F_g	Fecundity of individuals of breeding region g (mean number of offspring per pair)
p_g^{CMR}, $p_k^{LR,age}$, p_k^R	Recapture/recovery probabilities in breeding region g or non-breeding region k; age: for juveniles younger than 1 year (juv) and adults (ad)
σ_g	Standard deviation of the observation error for counts of breeding population g
Indices	
$g \in [1;G]$	Breeding regions
$k \in [1;K]$	Non-breeding regions
$t \in [1;T]$	Year since the beginning of the monitoring (dataset-specific)

multistate model by Korner-Nievergelt et al. (2014), it incorporates survival probabilities φ_k^{age} specific to non-breeding sites. The probability of recovering a dead individual in non-breeding region k t years after it had been marked in breeding region g is: $P_R(g,k,t) = m_{g,k} \times \varphi_k^{age\,t-1} \times \left(1 - \varphi_k^{age}\right) \times p_k^R$, where p_k^R is the probability of recovering the individual given it is in region k ($\varphi_k^{age} = \varphi_k^{juv}$ in the first year of an individual marked as juvenile, after which $\varphi_k^{age} = \varphi_k^{ad}$). Similar to the LR model, the likelihood of the dead-recovery model takes the form:

$$\prod_{g=1}^{G} Multinom(R_{g,(1:K)\times(1:T)}, Q_g \left| n_g^{Ringed}, m_{g,1:K}, \varphi_{1:K}^{age}, p_{1:K}^R \right.). \quad (2)$$

The third unit of the ICM fits data from tracking technologies (T) deployed on adults, with no data recovery bias other than survival, as is the generally case for GPS data. The model is again an adaptation of Arnason-Schwarz model by Korner-Nievergelt et al. (2017), which we have extended to correct for heterogeneous survival probabilities between non-breeding regions, similar to Rushing et al. (2021). We assumed that one trip is sufficient to identify the non-breeding site of a tagged individual and that tracking devices have no effect on the survival of the individuals. When there is no need to recapture individuals to collect the data, the proportion of tracks linking breeding region g and non-breeding region k reflects the transition probabilities between regions modulated by the probability that individuals survive their journey to non-breeding region k: $P_T(g,k) = m_{g,k} \times \varphi_k^{ad}$. Knowing the total number of tagged individuals in each breeding region n_g^{Tagged}, the likelihood of the tracking model takes the form:

$$\prod_{g=1}^{G} Multinom\left(T_{g,1:K} \left| n_g^{Tagged}, m_{g,1:K}, \varphi_{1:K}^{ad} \right.\right). \quad (3)$$

The fourth unit of the ICM fits capture–mark–recapture data (CMR) using a multinomial Cormack-Jolly-Seber framework (Cormack, 1964; Jolly, 1965; Seber, 1965). It aims at estimating annual survival Φ_g^{age} and recapture probabilities p_g^{CMR} from capture histories of individuals marked and reencountered alive within the breeding regions. However, following Rushing et al. (2021), migratory connectivity parameters can be involved through the average survival probabilities of individuals in breeding populations Φ_g^{age}, which can be expressed as the average survival probabilities during the non-breeding season φ_k^{age} weighted by the transition probabilities between breeding and non-breeding regions $m_{g,k}$:

$$\Phi_g^{age} = \sum_{k=1}^{K} m_{g,k} \times \varphi_k^{age}. \quad (4)$$

The probability of recapturing a marked individual of breeding population g last released in year t_C and recaptured in year t_R then is $P_{CMR}(t_C, t_R, g) = \Phi_g^{age\,t_R - t_C} \times \left(1 - p_g^{CMR}\right)^{t_R - t_C - 1} \times p_g^{CMR}$ ($\Phi_g^{age} = \Phi_g^{juv}$ in the first year of an individual marked as juvenile and $\Phi_g^{age} = \Phi_g^{ad}$ after). Similar to the LR model, knowing the total number of marked individuals in each breeding population n_g^{Ringed} over the t^{CMR} years of monitoring, the likelihood of the capture–mark–recapture model takes the form:

$$\prod_{g=1}^{G} \prod_{t_C=1}^{t^{CMR}} Multinom\left(CMR_{t_C,1:t_{CMR},g}, Q_g \middle| n_g^{Ringed,CMR}, \Phi_g^{age}, p_g^{CMR}\right). \quad (5)$$

When the total number of marked individuals n_g^{Ringed} or n_g^{Tagged} is not known, the same models units can be formulated by ignoring the probability of never recapturing/recovering data on marked individuals and scaling the rest of the probabilities to one (Procházka et al., 2017). Such models are not identifiable on their own, but can provide additional information when the parameters are also informed by other units of the integrated model for which the total number of marked individuals is known. As formulated above, the ICM relies on a set of assumptions. First, we assume fidelity of individuals to their breeding and non-breeding regions over the years. Migratory movements between breeding regions and non-breeding regions are set for every individual throughout its life. As such, migratory connectivity $m_{g,k}$ is assumed to be independent of age. Second, recapture and recovery probabilities are assumed to be homogeneous within each region k (or g) and annual survival is considered to depend solely on non-breeding regions, regardless of the origin of individuals. Last, all parameters are considered constant over the years. Each of these assumptions could be relaxed, and this base ICM could be generalised depending on the study system and the data available.

2.1.2 | Integrated population model (IPM)

The IPM aims to estimate demographic parameters for breeding populations, including annual survival Φ_g, fecundity F_g and the population size of breeding populations N_g while accounting for observation error. The IPM combines capture–mark–recapture data and breeding population counts without productivity data as exemplified in Kéry and Schaub (2012).

The first model unit of the IPM fits observed numbers of individuals based on the state-space framework of Kéry and Schaub (2012), although more complex population structures could be implemented. The biological process assumes two age classes in a pre-breeding survey: first year and adults older than 1 year. Individuals are assumed to start reproducing from their first year. Only breeding females are counted, which is equivalent to counting the number of breeding pairs. Assuming an even sex-ratio, first-year and adults have the same fecundity F_g and thus produce $F_g / 2$ juvenile females each year. Average survival probability for first-year and adults is Φ_g^{ad}, while juveniles have a different survival probability Φ_g^{juv}. All parameters are considered constant over the years.

The number of first-year in year $t + 1$ depends on the fecundity of first-year and adults, and the survival of juveniles to their first year, with demographic stochasticity modelled by a Poisson distribution:

$$N_{g,t+1}^{1} \sim Poisson\left(\left(N_{g,t}^{1} + N_{g,t}^{ad}\right) \times F_g / 2 \times \Phi_g^{juv}\right). \quad (6)$$

The number of adults in year $t + 1$ depends on the survival of first-year and adults, with demographic stochasticity modelled by a binomial distribution:

$$N_{g,t+1}^{ad} \sim Binomial\left(N_{g,t}^{1} + N_{g,t}^{ad}, \Phi_g^{ad}\right). \quad (7)$$

The observation process refers to an imperfect census of breeding females, with an observation error modelled as a normal error $\epsilon_{g,t} \sim Normal(0, \sigma_g)$:

$$N_{g,t}^{obs} = N_{g,t} + \epsilon_{g,t} = \left(N_{g,t}^{1} + N_{g,t}^{ad}\right) + \epsilon_{g,t}. \quad (8)$$

The second model unit of the IPM fits capture–mark–recapture data. It is identical to the fourth model unit in the ICM (Equation 5), except that the IPM can only identify Φ_g as a whole, not its components $m_{g,k}$ and φ_k (Equation 4).

2.1.3 | Integrated migratory connectivity and population model (ICPM)

The ICPM combines all previously described model units: the live-reencounter, the dead-recovery and the tracking models specific to the ICM, the population count model specific to the IPM and the capture–mark–recapture model shared by the ICM and the IPM, which is core to the ICPM. Through Equation (4), the data fed into the ICM informs Φ_g, a key parameter of the IPM, while the data fed into the IPM informs $m_{g,k}$, the central parameter of the ICM (Figure 1).

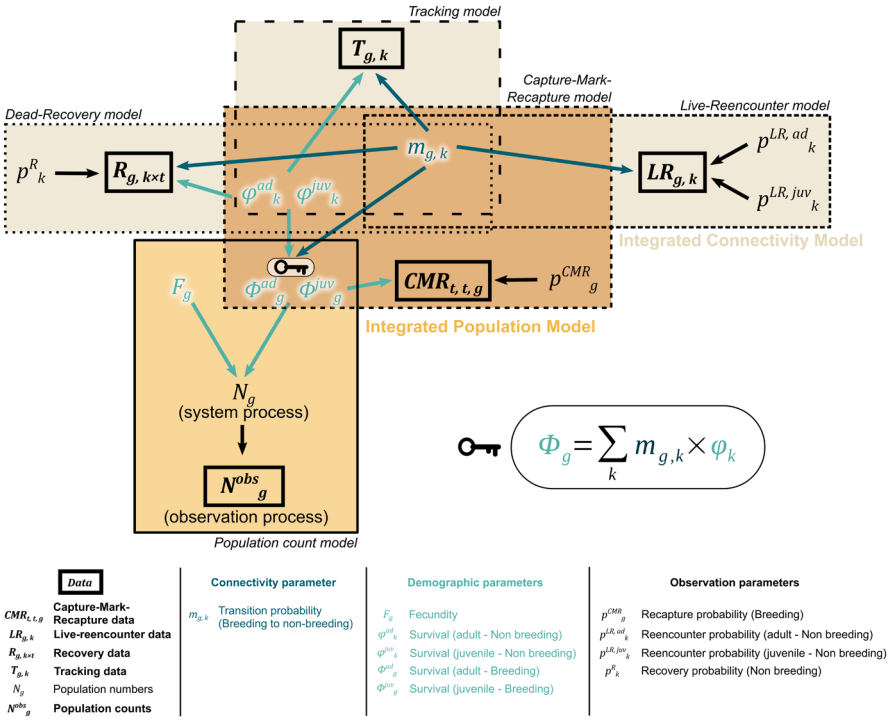

FIGURE 1 Graphical representation of the integrated connectivity and population model. Small boxes represent the data, large boxes represent the model units, arrows indicate the contribution of the parameters to the data in the models. The *key* formula for integrating both the integrated connectivity and the integrated population models relates survival probabilities for breeding populations Φ_g, survival probabilities in non-breeding regions φ_k and transition probabilities between breeding and non-breeding regions $m_{g,k}$.

2.2 | Model evaluation

2.2.1 | Data simulation

The performance of the models was evaluated using simulated data to check their ability to accurately estimate parameters with known values. We simulated 250 different datasets for each integrated model, using the same probabilistic processes as in the models (Equations 1–8). Each simulated dataset was composed of (1) dead-recoveries, live-reencounters and CMR data for individuals ringed as adults or juveniles in breeding regions, both when the total number of ringed individuals was known and unknown, (2) GPS data for individuals tagged as adults in breeding regions, both when the total number of tagged individuals was known and unknown and (3) breeding count data in a scenario where individuals participate in reproduction from their first year (Appendix S1 and code).

Each of these 250 simulated datasets was generated from an independent set of simulated parameter values for three breeding regions g and three non-breeding regions k. Connectivity parameters $m_{g,k}$ were drawn from a uniform distribution between 0.10 and 0.90 and normalised for each breeding region to generate transition probabilities between 5% and 80%. Recapture probabilities for live-reencounters and dead-recoveries in the non-breeding regions p_k^{LR} and p_k^{R} were drawn from a uniform distribution between 0.01 and 0.50, and between 0.05 and 0.75 for CMR data in the breeding regions p_g^{CMR} as recapture rates are typically higher in CMR designs than for opportunistic reencounters and recoveries. Annual adult survival probabilities in the non-breeding regions φ_k^{ad} were drawn from a uniform distribution between 0.25 and 0.90 to generate realistic survival rates that correspond to various life-history strategies and migration risks while avoiding drastic differences between non-breeding regions. These values were used to generate juvenile annual survival probabilities in the non-breeding regions φ_k^{juv}—set at about 50% of adult survival—and adult and juvenile annual survival probabilities for breeding populations Φ_g^{ad} and Φ_g^{juv}—using $m_{g,k}$ and Equation (4). To obtain a range of declining to increasing population trends while including a trade-off between survival and fecundity, we simulated annual fecundity F_g using a simple and arbitrary negative relationship with Φ_g^{ad}, set to produce annual growth rates roughly centred on 1 (Appendix S1). Only combinations of Φ_g^{ad} and F_g resulting in annual growth rates between 0.90 and 1.10 were retained to avoid population extinction or explosion over the simulated period. Initial population size for each breeding region was drawn from a normal distribution with mean 10,000 and standard deviation 500, and populations counts $N_{g,t}^{obs}$ were generated over 35 years with an observation error σ_g between 0 and 1000. In each breeding region, a total of 1000 individuals were ringed in the live-reencounter, dead-recovery and CMR datasets (100 per year for 10 years for the CMR data), and 50 individuals were tagged with GPS.

2.2.2 | Model assessment

The ICM and the IPM were compared with the ICPM, which combined these two integrated models into a single framework. Each of the three models was run on 250 simulated datasets. The relative bias of parameter estimates was calculated for the 250 runs as the difference between the estimated values and the simulated values

of the parameters, divided by the simulated values. The precision of parameter estimates was assessed from the mean and 95% confidence intervals of their coefficient of variation (CV) across the 250 runs, calculated as the standard deviation of estimates divided by their mean values.

2.3 | Case study: The Eurasian Curlew

2.3.1 | Study system

The Eurasian Curlew is a large migratory wader with a continuous distribution across Eurasia. It breeds from the British Isles to Siberia where it occupies a variety of inland and coastal wetlands, grasslands, cultivated fields and meadows. During the non-breeding season, its distribution shifts south from Western and South-Western Europe to Africa and South-Western Asia, where it is found mainly on the coast or near lakes and rivers with a high degree of site fidelity (Brown, 2015; del Hoyo et al., 1996). The species is considered near-threatened at the global scale (BirdLife International, 2021). In Europe, the subspecies *Numenius arquata arquata* shows contrasting estimated trends, as breeding populations are mostly declining while non-breeding populations seem to be increasing on the long term (Brown, 2015). While the main cause of decline for this long-lived species is suspected to be low breeding success due to intensive farming and predation pressures (Viana et al., 2023), its migratory dynamics are not well understood, which hampers comprehension of the links between breeding and non-breeding population dynamics.

2.3.2 | Delineation of breeding and non-breeding regions

We had to divide the continuous distribution range of the curlew in Europe into distinct populations or regions between which to investigate migratory connectivity. Three regions were delineated based on migration atlases (Bairlein et al., 2014; Bakken et al., 2003; Fransson et al., 2008; Saurola et al., 2013; Wernham et al., 2002): (1) a north-eastern region including Fennoscandia, the Baltic states and European Russia known to be a massive breeding source population; (2) a north-western region composed of Great-Britain and Ireland; and (3) a wide southern region stretching from Morocco and Spain to Turkey and extending as far north as Denmark (Figure 2). As these regions cover breeding and non-breeding grounds, we kept the same delineation for both seasons. We had no movement data for curlews migrating from Siberia or to the south of Morocco, limiting our analysis to the relative migratory connectivity between the three regions we defined. These regions were vast due to the resolution of our data, but offered a representative case study of large-scale heterogeneous datasets to illustrate the application of the integrated model. Dispersal movements between regions were considered negligible because they could not be distinguished from migratory movements just by looking at a breeding origin and a non-breeding destination of an individual. This assumption was consistent with the large size of the regions and the philopatric nature of the species.

2.3.3 | Migratory connectivity data

Connectivity data for the curlew included live-recaptures and dead-recoveries of individuals ringed between 2000 and 2017 extracted from the EURING databank (du Feu et al., 2016). We built 10 matrices summarising the number of individuals per ringing and reencounter regions (birds ringed as juveniles/adults × known/unknown number of ringed birds × live-recaptures/dead-recoveries, and birds ringed as adults × known/unknown number of ringed birds × CMR). To ensure the independence of the datasets, individuals who appeared in more than one dataset were filtered out, priority given to the dead-recovery, then the live-reencounter and finally the CMR datasets. GPS data was provided for 58 birds tagged between 2015 and 2021 during the breeding season in France, Germany, Finland and Estonia, with no information on the total number of tagged birds. The non-breeding region was identified from the most south-westerly location where the individuals were detected resting during the non-breeding season, further confirmed by visual inspection of the tracks.

2.3.4 | Breeding population data

Population count data were extracted from BirdLife International (2015), which presents estimates of the number of breeding pairs for each species and country in Europe around 1980 and 2012 with the corresponding population trends (BirdLife International, 2015). To homogenise count years between countries, for each country, population sizes around 2012 were first modelled as normal distributions by calculating the mean population size and estimating the standard deviation that would generate 95% of counts between the reported minimum and maximum. From these distributions, 100,000 values were sampled to project population counts in 1980 and 2012 using the median of reported population trends. We then summed the projected population counts across regions to produce a distribution of population sizes for each region in 1980 and 2012, the median of which was fitted as observed breeding population counts in the models. To help the models infer the population dynamics over this 32-year period, we also fitted annual growth rates calculated from the regional counts in 1980 and 2012, assuming that regional growth rates were constant over the study period since we had no data between these 2 years. The proportion of first-year in the initial population was calculated from a Leslie matrix based on previous estimates of survival and fecundity (Appendix S2). As curlews generally do not return to the breeding grounds in their first year (del Hoyo et al., 1996), we considered that first-year curlews were not reproducing and that the breeding count data informed only about the number of adult females ($N_t^{obs} = N_t^{ad}$) instead of

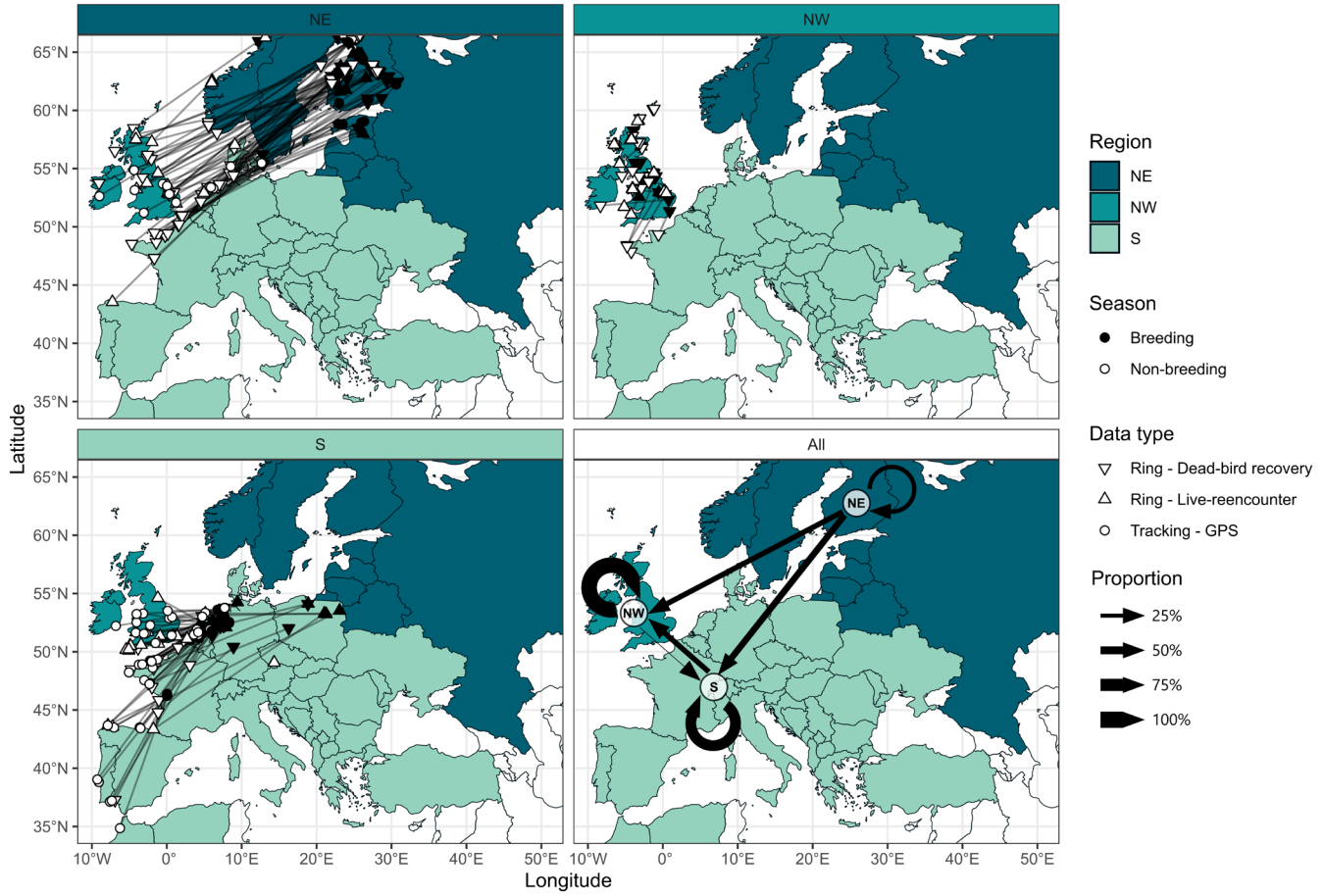

FIGURE 2 Migration network of the Eurasian Curlew in Europe. The three regions between which migratory movements have been investigated are shown in colour (NE: North-eastern Europe and western Russia; NW: North-western Europe; S: Southern Europe). Panels 'NE', 'NW' and 'S' split the data according to the breeding region of individuals. Lines connect the observations in the non-breeding region (white shapes) of individuals marked or tagged on their breeding grounds (black shapes), for ringing (triangles) and GPS data (circles). Panel 'All' summarises migration from breeding regions to non-breeding regions. The width of the arrows indicates the proportion of individuals moving from one breeding region to each non-breeding region.

the total number of adult and first-year females as in the general model ($N_t^{obs} = N_t^1 + N_t^{ad} + \epsilon_t$, Equation 8). Also, having only 2 years with population counts for each region did not allow us to explicitly model an observation error. The observation error ϵ_t was therefore confounded with the demographic stochasticity of N_t^{ad} (Equation 7) (Appendix S2).

2.3.5 | Licence information

The capture of curlews and GPS deployment in France was licenced by the CRBPO (French national ringing scheme) under the reference numbers PP1083 and PP336, in accordance with the animal experimentation guidelines of the EU Directive 2010/63/EU. In Germany, permission to tag curlews was granted by the Ministerium für Landwirtschaft, ländliche Räume, Europa und Verbraucherschutz of the federal state of Schleswig-Holstein (file numbers V 312–7224.121–37(42–3/13) and V 241–35,852/2017(88–7/17)), the Lower Saxony State Office for Consumer Protection and Food Safety (file numbers 33.19–42502–04–17/2699 and LAVES, AZ 33.19–42502-04–20/3373), and the State Agency for Nature, Environment and Consumer Protection of North Rhine-Westphalia (LANUV, AZ 81.02.04.2020.A097). Tagging in Estonia was carried out under the licence of the Matsalu Ringing Centre, Estonian Environmental Agency (file numbers 3-2013 and 4-2013 within the 'Programme of marking Eurasian curlew'). Permission to capture and tag curlews in Finland was granted by the Centre for Economic Development, Transport and the Environment (file numbers VARELY/1136/2020 and VARELY/3622/2017).

2.4 | Implementation of the models

Bayesian frameworks are flexible for assembling model units into integrated models. We implemented the integrated models in JAGS (Plummer, 2003) using R2jags package (Su & Yajima, 2020) in R 4.2.0 (R Core Team, 2022). Prior distributions of parameters were

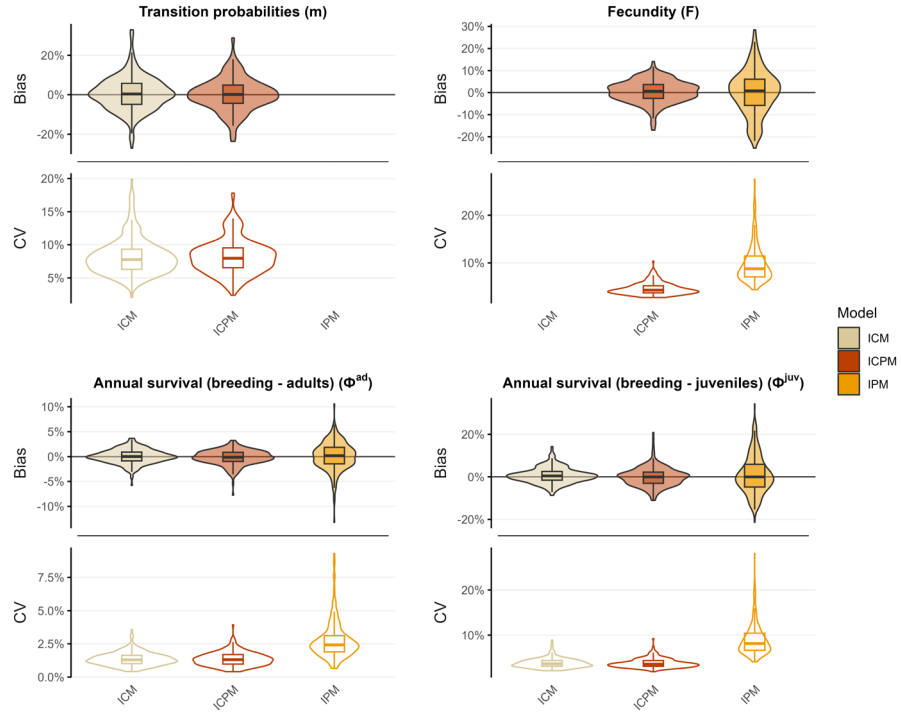

FIGURE 3 Relative bias and precision of parameter estimates for simulated data. Results are shown for the three integrated models: ICM, integrated connectivity model; ICPM, integrated connectivity and population model; IPM, integrated population model. Filled violin plots show the distribution of the relative bias of the estimates compared to the true values over the 250 simulations. White violin plots show the distribution of the coefficient of variation (CV) of the estimates over the 250 simulations as a proxy for their precision. For each family of parameter—transition probabilities, fecundity, survival (adults) and survival (juveniles)—parameters showed the same pattern irrespective of the breeding and/or non-breeding region. Therefore, only one representative parameter for each family has been presented here as a summary, that is $m_{1,1}$, F_1, Φ_1^{ad} and Φ_1^{juv}, even if general results are described in the main text. Results for the remaining parameters are presented in Appendix S3.

non-informative, corresponding to uniform distributions between 0 and 1 for all probabilities and between 0 and 6 for fecundity. For the curlew, the lack of CMR data for juveniles did not allow the IPM to disentangle juvenile survival and fecundity. Therefore, uniform priors for juvenile survival were restricted between 0.35 and 0.50 in the IPM based on previous estimates from the literature to improve model convergence (Appendix S2) (Viana et al., 2023). The integrated models were run for about 1,000,000 iterations, until convergence of MCMC chains, using a Gelman-Rubin convergence diagnostic Rhat of less than 1.1 and an effective sample size greater than 100 as a sign of convergence, confirmed by visual inspection of the trace plots (Gelman & Rubin, 1992).

3 | RESULTS

3.1 | Performance of the integrated models on simulated data

On average, the integrated connectivity and population model 'ICPM' and the integrated connectivity model 'ICM' showed no bias and similar CV for transition probabilities m (i.e. connectivity parameters; median $bias^{ICM}_{m} \approx$ median $bias^{ICPM}_{m} = 0.1\%$ [95% quantile range: −15.6%–16.8%]; median $CV^{ICM}_{m} \approx$ median $CV^{ICPM}_{m} = 8.0\%$ [QR: 3.7%–13.9%]) (Figure 3; Appendix S3). The same behaviour of the models could be observed for adult and juvenile breeding survival estimates Φ_{ad} and Φ_{juv}, although the distribution ranges suggest that the magnitude of bias was smaller for the ICPM and the ICM than for the integrated population model 'IPM' (e.g. for adults: median $bias^{ICM}_{\Phi} \approx$ median $bias^{ICPM}_{\Phi} = -0.1\%$ [QR: −3.4%–2.4%], less dispersed than $bias^{IPM}_{\Phi}$ with median 0.2% and QR −6.2%–5.1%). The ICPM and the ICM also performed twice better than the IPM in terms of precision (e.g. for adults: median $CV^{ICM}_{\Phi} \approx$ median $CV^{ICPM}_{\Phi} = 1.3\%$ [QR: 0.6%–2.5%] < median $CV^{IPM}_{\Phi} = 2.4\%$ [QR: 1.0%–6.2%]). Compared to the IPM, the ICPM allowed the estimation of fecundity F with higher precision (median $CV^{ICPM}_{F} = 4.3\%$ [QR: 3.0%–7.7%] < median $CV^{IPM}_{F} = 8.8\%$ [QR: 5.5%–21.4%]). The extent of bias distributions suggests that the magnitude of bias was also lower for fecundity estimates produced by the ICPM compared to those of the IPM (median $bias^{ICPM}_{F} = 0.6\%$ [QR: −10.6%–8.6%]; median $bias^{IPM}_{F} = 0.8\%$ [QR: −19.3%–20.1%]).

3.2 | Application to the Eurasian Curlew

Applied to the Curlew data, the integrated connectivity model 'ICM' and the integrated connectivity and population model 'ICPM'

produced similar estimates for transition probabilities $m_{g,k}$, except for the probability of curlews breeding in the NE region to overwinter in the same region for $m_{NE,NE}$, which was significantly reduced in the ICPM ($m^{ICPM}_{NE,NE}$ =0.12 [95% Credible Interval: 0.04–0.25] < $m^{ICM}_{NE,NE}$ =0.43 [CI: 0.30–0.57]; Figure 4). Both models suggested a diffuse migration from the NE region, with a probability of $m^{ICPM}_{NE,NW}$ =0.42 [CI: 0.29–0.57] for curlews to migrate towards the NW region, and $m^{ICPM}_{NE,S}$ =0.45 [CI: 0.28–0.62] for curlews to migrate towards the S region. Curlews breeding in the NW and S regions showed a strong tendency to remain in the same region during the non-breeding season, with probabilities of $m^{ICPM}_{NW,NW}$ =0.91 [CI: 0.81–0.97] and $m^{ICPM}_{S,S}$ =0.72 [CI: 0.60–0.82].

Concerning demographic parameters estimates, average annual survival of both adults and juveniles from the breeding region, Φ^{ad}_g and Φ^{juv}_g, were higher and more precise in the ICPM compared to the ICM (Figure 4). Adult survival estimates Φ^{ad}_g in the integrated population model 'IPM' were similar to the ICPM, but juvenile survival Φ^{juv}_g had to be constrained to allow the IPM to converge and is therefore not comparable to the estimates of the two other models. Similarly, the ICPM was able to estimate fecundity F_g without

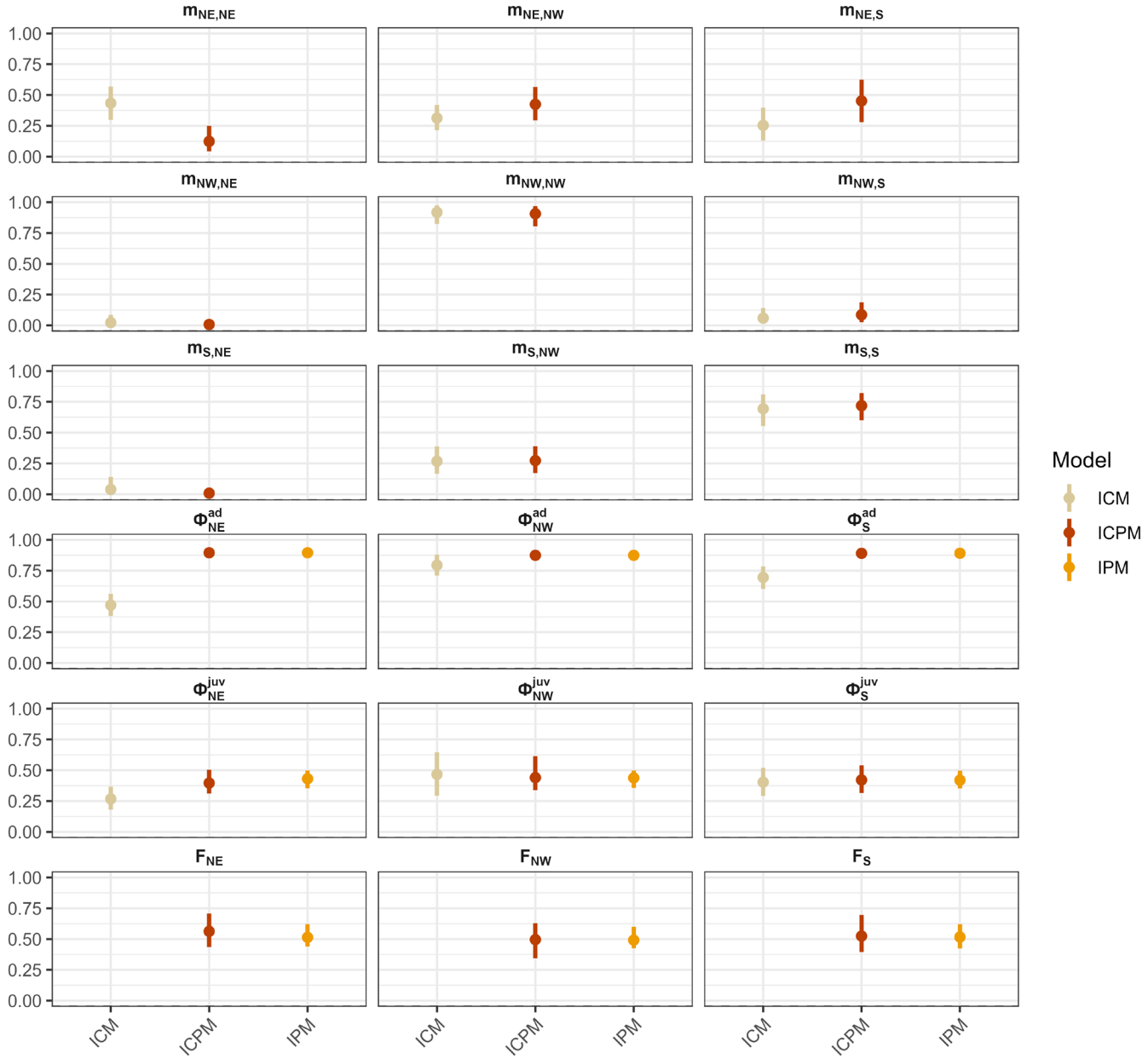

FIGURE 4 Migratory connectivity and demographic estimates for the Eurasian Curlew in Europe. Mean values and 95% credible intervals (CI) are displayed for estimates of migratory connectivity ($m_{g,k}$), annual survival of breeding populations for adults and juveniles (Φ^{ad}_g and Φ^{juv}_g, respectively), and fecundity (F_g). Indices correspond to breeding regions g and non-breeding regions k (NE: North-eastern Europe and western Russia; NW: North-western Europe; S: Southern Europe). The three integrated models are compared for each parameter (ICM, integrated connectivity model; ICPM, integrated connectivity and population model; IPM, integrated population model).

needing juvenile survival to be fixed, contrary to the IPM. According to the ICPM, adult survival was slightly lower in the NW region $\Phi^{ad}_{NW} = 0.874$ [CI: 0.872–0.877] compared to the NE and S regions where $\Phi^{ad}_{NE} \approx \Phi^{ad}_{S} = 0.890$ [CI: 0.884–0.896]. Juvenile survival and fecundity were analogous between all regions as all credible intervals overlapped: $\Phi^{juv}_{NE} \approx \Phi^{juv}_{NW} \approx \Phi^{juv}_{S} = 0.42$ [CI: 0.31–0.54] and $F_{NE} \approx F_{NW} \approx F_{S} = 0.52$ [CI: 0.40–0.70].

4 | DISCUSSION

We provided an example of an integrated connectivity and population model that combines existing model units from both fields of migratory connectivity and population dynamics, allowing the sharing of information on migration movements and demographics. Tested on comprehensive simulated data, the ICPM estimated transition probabilities between breeding and non-breeding regions with no bias and similar precision to the ICM. The integration of connectivity and population data mainly enhanced the precision of demographic parameters compared to an IPM without productivity data. However, when applied to a real dataset for the curlew, the ICPM improved the estimation of transition and survival probabilities for some regions compared to the ICM, and was better able than the IPM to cope with the lack of CMR data that hindered the identification of juvenile survival and fecundity. Improved precision of estimates and the ability to estimate parameters not directly informed by the data are two key features of integrated population models (Abadi, Gimenez, Ullrich, et al., 2010; Besbeas et al., 2002; Schaub & Abadi, 2011) and integrated migratory connectivity models (Korner-Nievergelt et al., 2017; Procházka et al., 2017; Von Rönn et al., 2020) that have successfully propagated in our model, provided the connectivity and population datasets are sufficiently complete or complementary to inform all but at most one parameter of the ICM and the IPM.

In this study, the improvement in precision generally did not concern the migratory connectivity estimates despite the link created between these parameters and the population count data through the integration (Equation 4). This resulted from the larger amount of connectivity data compared to demographic data, especially the dead-recovery data that informed survival in the non-breeding regions and was quite abundant for the curlew as it is a game species in some countries (Appendix S3). In the simulation analysis, it enabled the ICM to produce well-supported connectivity estimates and survival estimates with higher precision than the IPM. For the curlew, integrating dead-recoveries in the non-breeding season through the ICM was necessary to estimate juvenile survival, which could not be achieved by the IPM alone due to the lack of CMR data for juveniles. The integration of connectivity and population models allowed this precise information on adult and juvenile survival to be fed into the population model, where it improved its ability to disentangle survival and fecundity from growth rates, ultimately making fecundity estimable or more precise.

We would expect population data to have a stronger influence on connectivity estimates if it was more comprehensive than migratory connectivity data. For the curlew, the population model constrained survival to fit population count data, resulting in a higher survival estimate and a lower migratory connectivity for individuals breeding in the NE region via Equation (4). Indeed, dead-recovery data was limiting in the NE region, preventing a reliable estimation of non-breeding survival for this region (Appendices S2 and S4). Adding information on population trends constrained breeding survival in the NE region to a higher value, and since survival in the other non-breeding regions was better informed, the model rebalanced connectivity and non-breeding survival in the NE region to more realistic values—although this conflicting information between two sparse datasets led to a convergence harder to achieve for juvenile survival, the least informed parameter, in the ICPM compared to the ICM. The ICM and the IPM integrate datasets that inform about different groups of processes, and the intersection of these different points of view resulted in the observed improvement in the precision of estimates.

More generally, combining data from both breeding and non-breeding seasons in the ICPM provides more information on region-specific survival and recapture probabilities as demographic processes in the different regions are connected. This may allow the estimation of demographic parameters for regions with scarce data, as was the case for the NE region in the curlew application. We expect this sharing of information to be particularly relevant when survival and recapture probabilities are heterogeneous across regions (Lebreton & Pradel, 2002), and when migratory connectivity is strong, making some breeding regions more dependent on some non-breeding regions (Webster et al., 2002). In such situations, the integrated model should better identify the contribution of each non-breeding season to the dynamics of each breeding season (and vice-versa) compared to independent migratory connectivity or population dynamics models, resulting in a more precise description of inter-regional heterogeneity.

Even for a simple application to the curlew, the ICPM provided estimates coherent with previous descriptions of its migratory patterns and demographic parameters. Consistently with migratory atlases, our migratory connectivity estimates advocate for a diffuse migration of birds from Russian and Scandinavian populations towards Great-Britain and south-western Europe, while birds of north-western and Southern Europe tend to stay in the same regions during the breeding and non-breeding seasons (Bairlein et al., 2014; Bakken et al., 2003; Fransson et al., 2008; Saurola et al., 2013; Wernham et al., 2002). Our estimates of annual adult survival for the different breeding populations were also consistent with previous European-scale studies (Méndez et al., 2018; Roodbergen et al., 2012; Viana et al., 2023). Juvenile survival and fecundity were similar to previous estimates, with fecundity still low enough to corroborate the hypothesis that low breeding success may be driving population declines in all three regions of Europe. However, the contribution of population counts to the estimation of demographic parameters may be slightly biased in this particular example, as we were not able to account for observation errors due to the scarcity of our data. Additionally, the size of our regions and the resolution of our analysis

do not allow us to draw conclusions about finer-scale movements within the regions, as curlews are known to move closer to shores during the non-breeding season (del Hoyo et al., 1996). Also, it is impossible to assess how much our estimates are affected by the lack of data for birds breeding in the large Siberian populations or migrating to unmonitored regions outside Europe, which still hinders our understanding of why breeding and non-breeding populations in Europe show distinct trends. A more detailed analysis with complementary data collected at various points in the curlew's annual cycle would be required to fully understand its population dynamics.

Studies on migratory species typically bring together datasets from different parts of a species' annual cycle through international collaborations, which may differ in spatiotemporal coverage or sampling effort. Integrated modelling thus offers two additional benefits for the study of migratory species. First, despite being data demanding, the ICPM confronts the strengths and weaknesses of various datasets, compensating for some of their imbalances (Saunders et al., 2019; Zipkin et al., 2019). Second, as a distribution of migratory connectivity values is being estimated concurrently with demographic parameters, an integrated framework such as the one presented here propagates uncertainty between connectivity patterns and demographic processes (Schaub & Abadi, 2011), which may nuance the conclusions of studies about the impact of localised events in the migration network (e.g. Hallworth et al., 2021). Yet, combining migratory connectivity data and population dynamics data in the ICPM raises new challenges. Current studies generally consider migratory connectivity patterns to be static, whereas population sizes are time-dependent. Individuals may change their migratory behaviour in response to environmental changes (Fiedler et al., 2004), or face differential selection on a migration route (Hewson et al., 2016), resulting in changes in migratory connectivity over time. Ignoring such changes may bias survival and fecundity estimates of the population model. If sufficient data are available, migratory connectivity could be allowed to vary over time as population sizes do, shedding additional light on the dependence of migration patterns on population dynamics.

The integrated model we presented uses model units from recent connectivity and population studies. Each unit could be further developed to improve the performance of the integrated model. First, depending on the available data, survival and detection probabilities may need to be modelled more specifically. The tracking model could account for the effect of tags on survival and include a tag-recapture probability, in order to avoid underestimating non-breeding survival. This would notably make the model more appropriate to analyse data from archival tags such as geolocators (Rushing et al., 2021). In the live-reencounter model, reencounter probabilities were not informed by any other dataset and absorbed heterogeneities between non-breeding regions, including the variance due to survival (Korner-Nievergelt et al., 2010). However, a similar structure to the dead-recovery model could be adopted to disentangle survival and ring-resighting probabilities, so that live-reencounter data also informs survival in the non-breeding regions (Cohen et al., 2014). With the appropriate data (repeated counts for each year), the observation error of the population count model could also be modelled as country- or region-specific detection probabilities, allowing to further account for heterogeneities between regions in monitoring (Kéry & Schaub, 2012). Second, the model units we used consider migratory movements between clearly identified populations. For species with a continuous distribution range, methodologies to identify meaningful units within their distribution range, or the inclusion of continuous-space approaches would be beneficial (Hobson et al., 2014; Schirmer et al., 2023). This would release assumptions about homogeneous recapture probabilities within regions (Korner-Nievergelt et al., 2017) and make transition probabilities and demographic estimates more informative than in a large-scale diffuse system. Third, we did not consider dispersal between regions. For species exhibiting dispersal, a population or capture–mark–recapture model incorporating dispersal parameters should be necessary to obtain unbiased estimates of migratory connectivity. Dispersal might be particularly important to consider when investigating migratory connectivity between smaller regions, a scale at which movements between breeding regions can be detectable and quantitatively affect migratory connectivity. Finally, individual or environmental covariates affecting migration movements, population numbers, fecundity and/or survival in the breeding and non-breeding seasons could be added to bridge the gap with full-annual cycle models (Hostetler et al., 2015).

Producing unbiased estimates of migratory connectivity and region-specific demographic parameters with improved precision when data are scarce, the ICPM provides a novel perspective to investigate the interaction between migration and demographic patterns. The framework we present is built on tools that exist in both fields of migratory connectivity and population dynamics. Our example of ICPM combines various migratory connectivity data for illustration purpose, but in most cases a reduced form may provide most of the observed benefits of the integrated model. For instance, dead-recovery data in the non-breeding regions would likely provide much of the observed improvement in breeding survival and fecundity estimates for species with high, homogeneous mortality and recovery rates. The flexibility of this framework also allows the modelling of diverse population structures, and the inclusion of various data already integrated in either field, including isotope or genetic signatures that provide information on migratory connectivity at large-scale (Ruegg et al., 2017; Von Rönn et al., 2020) or productivity data from breeding monitoring (Abadi, Gimenez, Ullrich, et al., 2010). The possibilities offered by such a flexible framework provide food for thought for the collection of migratory connectivity data (Hobson et al., 2014), which could be complemented by the collection of environmental and demographic data throughout the migration cycle.

AUTHOR CONTRIBUTIONS

Killian A. Gregory, Aurélien Besnard, Charlotte Francesiaz and Frédéric Jiguet conceptualised the study. Jaanus Elts, Riho Marja, Pierrick Bocher, Heinz Düttmann, Thomas Fartmann, Stefan Garthe, Steffen Kämpfer, Helmut Kruckenberg, Markus Piha and Philipp

Schwemmer collected the GPS data for the Eurasian Curlew. Killian A. Gregory developed the model, analysed the data and wrote the manuscript. All authors contributed to the drafts and gave final approval for publication.

ACKNOWLEDGEMENTS

We are thankful to Marc Kéry, whose suggestions on the early stages of the manuscript were invaluable, and to three anonymous reviewers for their insightful comments that helped to improve the manuscript. We are particularly grateful to EURING, which made the ringing data available, to the ringers and ringing scheme staff members who have gathered and prepared the data, and to the BTO for kindly sharing their records of ringing totals.

FUNDING INFORMATION

The BTO Ringing Scheme is funded by a partnership of the British Trust for Ornithology, the Joint Nature Conservation Committee (on behalf of: Natural England, Natural Resources Wales and Scottish Natural Heritage and the Department of the Environment Northern Ireland), The National Parks and Wildlife Service (Ireland) and the ringers themselves. Data collection in France was funded by the Contrat de Plan Etat-Région and the CNRS (ECONAT project), the European Regional Development Fund (QUALIDRIS project), the Ligue pour la Protection des Oiseaux and the French Ministry of Ecology (BirdMan project). In Germany, funding was provided by the German Federal Agency for Nature Conservation (Bundesamt für Naturschutz, BfN, grant no. FKZ 3520532052) with funds from the Federal Ministry for the Environment, Nature Conservation and Nuclear Safety (BMU) within the projects 'Birdmove' (grant no. FKZ 3515822100) and 'Trackbird' (grant no. FKZ 3519861400), the Lower Saxonian Wadden Sea Foundation ('Niedersächsische Wattenmeerstiftung') and the District of Aurich. Tagging in Estonia was carried out as part of the 'Applied research for conservation of the Eurasian curlew' funded by the Estonian Environmental Investment Centre (grant no. 8172). This study is part of the HABITRACK project funded by the European Union through its HORIZON Research and Innovation Actions (Project 101135047, HORIZON-CL6-2023-BIODIV-01—Biodiversity and Ecosystem Services).

CONFLICT OF INTEREST STATEMENT

The authors declare no conflicts of interest.

PEER REVIEW

The peer review history for this article is available at https://www.webofscience.com/api/gateway/wos/peer-review/10.1111/2041-210X.14489.

DATA AVAILABILITY STATEMENT

Processed data and code to reproduce the study are available on Zenodo at https://doi.org/10.5281/zenodo.14245333 (Gregory, 2024). For Eurasian Curlew data, original data from EURING can be requested on their website https://euring.org/, ringing totals for Great Britain can be requested from the BTO on their website https://www.bto.org/, population counts from BirdLife international are available from the *European Red List of Birds* (2015), and GPS data are archived on the Movebank platform (movebank.org) under the ID numbers 1077731101, 1126572166 and 325569416.

ORCID

Killian A. Gregory https://orcid.org/0000-0002-0316-5041
Charlotte Francesiaz https://orcid.org/0000-0002-2944-695X
Frédéric Jiguet https://orcid.org/0000-0002-0606-7332
Pierre-André Crochet https://orcid.org/0000-0002-0422-3960
Pierrick Bocher https://orcid.org/0000-0001-7751-5844
Heinz Düttmann https://orcid.org/0000-0003-4764-5474
Jaanus Elts https://orcid.org/0000-0002-2672-4918
Thomas Fartmann https://orcid.org/0000-0002-2050-9221
Stefan Garthe https://orcid.org/0000-0003-0548-9346
Steffen Kämpfer https://orcid.org/0000-0002-1746-3453
Helmut Kruckenberg https://orcid.org/0000-0003-3840-1240
Riho Marja https://orcid.org/0000-0002-9390-6201
Markus Piha https://orcid.org/0000-0002-8482-6162
Philipp Schwemmer https://orcid.org/0000-0002-3930-2845
Aurélien Besnard https://orcid.org/0000-0002-2289-9761

REFERENCES

Abadi, F., Gimenez, O., Arlettaz, R., & Schaub, M. (2010). An assessment of integrated population models: Bias, accuracy, and violation of the assumption of independence. *Ecology*, *91*(1), 7–14. https://doi.org/10.1890/08-2235.1

Abadi, F., Gimenez, O., Ullrich, B., Arlettaz, R., & Schaub, M. (2010). Estimation of immigration rate using integrated population models. *Journal of Applied Ecology*, *47*(2), 393–400. https://doi.org/10.1111/j.1365-2664.2010.01789.x

Bairlein, F., Dierschke, J., Dierschke, V., Salewski, V., Geiter, O., Hüppop, K., Köppen, U., & Fiedler, W. (2014). *Atlas des Vogelzugs*. AULA-Verlag.

Bakken, V., Runde, O., & Tjørve, E. (2003). *Norsk ringmerkingsatlas* (Vol. *1*). Natur og Fritid.

Besbeas, P., Freeman, S. N., Morgan, B. J. T., & Catchpole, E. A. (2002). Integrating mark–recapture–recovery and census data to estimate animal abundance and demographic parameters. *Biometrics*, *58*(3), 540–547. https://doi.org/10.1111/j.0006-341X.2002.00540.x

BirdLife International. (2015). *European red list of birds*. Office for Official Publications of the European Communities.

BirdLife International. (2021). *IUCN red list for birds*. http://www.birdlife.org

Brown, D. J. (2015). *International Single Species Action Plan for the conservation of the Eurasian Curlew Numenius arquata arquata, N. a. Orientalis and N. a. Suschkini*. (58; AEWA Technical Series).

Cohen, E. B., Hostetler, J. A., Royle, J. A., & Marra, P. P. (2014). Estimating migratory connectivity of birds when re-encounter probabilities are heterogeneous. *Ecology and Evolution*, *4*(9), 1659–1670. https://doi.org/10.1002/ece3.1059

Cormack, R. M. (1964). Estimates of survival from the sighting of marked animals. *Biometrika*, *51*(3/4), 429–438. https://doi.org/10.2307/2334149

del Hoyo, J., Elliot, A., & Sargatal, J. (1996). *Handbook of the birds of the world: Vol. 3: Hoatzin to Auks*. Lynx Ediction.

du Feu, C. R., Clark, J. A., Schaub, M., Fiedler, W., & Baillie, S. R. (2016). The EURING Data Bank—A critical tool for continental-scale studies of marked birds. *Ringing & Migration*, *31*(1), 1–18. https://doi.org/10.1080/03078698.2016.1195205

Dunn, D. C., Harrison, A.-L., Curtice, C., DeLand, S., Donnelly, B., Fujioka, E., Heywood, E., Kot, C. Y., Poulin, S., Whitten, M., Åkesson, S., Alberini, A., Appeltans, W., Arcos, J. M., Bailey, H., Ballance, L. T., Block, B., Blondin, H., Boustany, A. M., … Halpin, P. N. (2019). The importance of migratory connectivity for global ocean policy. *Proceedings of the Royal Society B: Biological Sciences*, *286*(1911), 20191472. https://doi.org/10.1098/rspb.2019.1472

Fiedler, W., Bairlein, F., & Köppen, U. (2004). Using large-scale data from ringed birds for the investigation of effects of climate change on migrating birds: Pitfalls and prospects. *Advances in Ecological Research*, *35*, 49–67. https://doi.org/10.1016/S0065-2504(04)35003-8

Finch, T., Butler, S. J., Franco, A. M. A., & Cresswell, W. (2017). Low migratory connectivity is common in long-distance migrant birds. *Journal of Animal Ecology*, *86*(3), 662–673. https://doi.org/10.1111/1365-2656.12635

Fransson, T., Österblom, H., & Hall-Karlsson, S. (2008). *Svensk ringmärkningatlas* (Vol. *2*). ONCFS.

Gao, B., Hedlund, J., Reynolds, D. R., Zhai, B., Hu, G., & Chapman, J. W. (2020). The 'migratory connectivity' concept, and its applicability to insect migrants. *Movement Ecology*, *8*(1), 48. https://doi.org/10.1186/s40462-020-00235-5

Gelman, A., & Rubin, D. B. (1992). Inference from iterative simulation using multiple sequences. *Statistical Science*, *7*(4), 457–472.

Gregory, K. A. (2024). Data from: An integrative framework to combine migratory connectivity and demographic data—Processed data and code. *Zenodo*, https://doi.org/10.5281/zenodo.14245333

Gregory, K. A., Francesiaz, C., Jiguet, F., & Besnard, A. (2023). A synthesis of recent tools and perspectives in migratory connectivity studies. *Movement Ecology*, *11*(1), 69. https://doi.org/10.1186/s40462-023-00388-z

Hallworth, M. T., Bayne, E., McKinnon, E., Love, O., Tremblay, J. A., Drolet, B., Ibarzabal, J., Van Wilgenburg, S. L., & Marra, P. P. (2021). Habitat loss on the breeding grounds is a major contributor to population declines in a long-distance migratory songbird. *Proceedings of the Royal Society B: Biological Sciences*, *288*, 20203164. https://doi.org/10.1098/rspb.2020.3164

Harrison, X. A., Blount, J. D., Inger, R., Norris, D. R., & Bearhop, S. (2011). Carry-over effects as drivers of fitness differences in animals. *Journal of Animal Ecology*, *80*(1), 4–18. https://doi.org/10.1111/j.1365-2656.2010.01740.x

Hewson, C. M., Thorup, K., Pearce-Higgins, J. W., & Atkinson, P. W. (2016). Population decline is linked to migration route in the Common Cuckoo. *Nature Communications*, *7*(1), 12296. https://doi.org/10.1038/ncomms12296

Hobson, K. A., Van Wilgenburg, S. L., Faaborg, J., Toms, J. D., Rengifo, C., Sosa, A. L., Aubry, Y., & Aguilar, R. B. (2014). Connecting breeding and wintering grounds of Neotropical migrant songbirds using stable hydrogen isotopes: A call for an isotopic atlas of migratory connectivity. *Journal of Field Ornithology*, *85*(3), 237–257. https://doi.org/10.1111/jofo.12065

Hostetler, J. A., Sillett, T. S., & Marra, P. P. (2015). Full-annual-cycle population models for migratory birds. *The Auk*, *132*(2), 433–449. https://doi.org/10.1642/AUK-14-211.1

Jiguet, F., Robert, A., Lorrillière, R., Hobson, K. A., Kardynal, K. J., Arlettaz, R., Bairlein, F., Belik, V., Bernardy, P., Copete, J. L., Czajkowski, M. A., Dale, S., Dombrovski, V., Ducros, D., Efrat, R., Elts, J., Ferrand, Y., Marja, R., Minkevicius, S., … Moussy, C. (2019). Unravelling migration connectivity reveals unsustainable hunting of the declining ortolan bunting. *Science Advances*, *5*(5), eaau2642. https://doi.org/10.1126/sciadv.aau2642

Jolly, G. M. (1965). Explicit estimates from capture-recapture data with both death and immigration-stochastic model. *Biometrika*, *52*(1/2), 225–247. https://doi.org/10.2307/2333826

Kéry, M., & Schaub, M. (2012). *Bayesian population analysis using WinBUGS: A hierarchical perspective* (1st ed.). Academic Press.

Korner-Nievergelt, F., Liechti, F., & Thorup, K. (2014). A bird distribution model for ring recovery data: Where do the European robins go? *Ecology and Evolution*, *4*(6), 720–731. https://doi.org/10.1002/ece3.977

Korner-Nievergelt, F., Prévot, C., Hahn, S., Jenni, L., & Liechti, F. (2017). The integration of mark reencounter and tracking data to quantify migratory connectivity. *Ecological Modelling*, *344*, 87–94. https://doi.org/10.1016/j.ecolmodel.2016.11.009

Korner-Nievergelt, F., Sauter, A., Atkinson, P. W., Guélat, J., Kania, W., Kéry, M., Köppen, U., Robinson, R. A., Schaub, M., Thorup, K., van der Jeugd, H., & van Noordwijk, A. J. (2010). Improving the analysis of movement data from marked individuals through explicit estimation of observer heterogeneity. *Journal of Avian Biology*, *41*(1), 8–17. https://doi.org/10.1111/j.1600-048X.2009.04907.x

Lebreton, J. D., & Pradel, R. (2002). Multistate recapture models: Modelling incomplete individual histories. *Journal of Applied Statistics*, *29*(1–4), 353–369. https://doi.org/10.1080/02664760120108638

Marra, P. P., Cohen, E. B., Loss, S. R., Rutter, J. E., & Tonra, C. M. (2015). A call for full annual cycle research in animal ecology. *Biology Letters*, *11*(8), 20150552. https://doi.org/10.1098/rsbl.2015.0552

Marra, P. P., Hobson, K. A., & Holmes, R. T. (1998). Linking winter and summer events in a migratory bird by using stable-carbon isotopes. *Science*, *282*(5395), 1884–1886. https://doi.org/10.1126/science.282.5395.1884

Méndez, V., Alves, J. A., Gill, J. A., & Gunnarsson, T. G. (2018). Patterns and processes in shorebird survival rates: A global review. *Ibis*, *160*(4), 723–741. https://doi.org/10.1111/ibi.12586

Myers, J. P. (1981). Cross-seasonal interactions in the evolution of sandpiper social systems. *Behavioral Ecology and Sociobiology*, *8*(3), 195–202. https://doi.org/10.1007/BF00299830

Norevik, G., Åkesson, S., Artois, T., Beenaerts, N., Conway, G., Cresswell, B., Evens, R., Henderson, I., Jiguet, F., & Hedenström, A. (2020). Wind-associated detours promote seasonal migratory connectivity in a flapping flying long-distance avian migrant. *Journal of Animal Ecology*, *89*(2), 635–646. https://doi.org/10.1111/1365-2656.13112

Norris, D. R., & Marra, P. P. (2007). Seasonal interactions, habitat quality, and population dynamics in migratory birds. *The Condor*, *109*(3), 535–547. https://doi.org/10.1093/condor/109.3.535

Plummer, M. (2003). *JAGS: A program for analysis of Bayesian graphical models using Gibbs sampling*. Working Papers.

Procházka, P., Hahn, S., Rolland, S., van der Jeugd, H., Csörgő, T., Jiguet, F., Mokwa, T., Liechti, F., Vangeluwe, D., & Korner-Nievergelt, F. (2017). Delineating large-scale migratory connectivity of reed warblers using integrated multistate models. *Diversity and Distributions*, *23*(1), 27–40. https://doi.org/10.1111/ddi.12502

R Core Team. (2022). *R: A language and environment for statistical computing* [computer software]. R Foundation for Statistical Computing. https://www.R-project.org/

Roodbergen, M., van der Werf, B., & Hötker, H. (2012). Revealing the contributions of reproduction and survival to the Europe-wide decline in meadow birds: Review and meta-analysis. *Journal of Ornithology*, *153*(1), 53–74. https://doi.org/10.1007/s10336-011-0733-y

Ruegg, K. C., Anderson, E. C., Harrigan, R. J., Paxton, K. L., Kelly, J. F., Moore, F., & Smith, T. B. (2017). Genetic assignment with isotopes and habitat suitability (GAIAH), a migratory bird case study. *Methods in Ecology and Evolution*, *8*(10), 1241–1252. https://doi.org/10.1111/2041-210X.12800

Runge, C. A., Martin, T. G., Possingham, H. P., Willis, S. G., & Fuller, R. A. (2014). Conserving mobile species. *Frontiers in Ecology and the Environment*, *12*(7), 395–402. https://doi.org/10.1890/130237

Rushing, C. S., Van Tatenhove, A. M., Sharp, A., Ruiz-Gutierrez, V., Freeman, M. C., Sykes, P. W., Given, A. M., & Sillett, T. S. (2021). Integrating tracking and resight data enables unbiased inferences

about migratory connectivity and winter range survival from archival tags. *Ornithological Applications*, *123*(2), duab010. https://doi.org/10.1093/ornithapp/duab010

Saunders, S. P., Farr, M. T., Wright, A. D., Bahlai, C. A., Ribeiro, J. W., Rossman, S., Sussman, A. L., Arnold, T. W., & Zipkin, E. F. (2019). Disentangling data discrepancies with integrated population models. *Ecology*, *100*(6), e02714. https://doi.org/10.1002/ecy.2714

Saurola, P., Valkama, J., & Velmala, W. (2013). *The Finnish Bird Ringing Atlas* (Vol. *1*). Finnish Museum of Natural History and Ministry of Environment.

Schaub, M., & Abadi, F. (2011). Integrated population models: A novel analysis framework for deeper insights into population dynamics. *Journal of Ornithology*, *152*(1), 227–237. https://doi.org/10.1007/s10336-010-0632-7

Schirmer, S., Korner-Nievergelt, F., von Rönn, J. A. C., & Liebscher, V. (2023). Estimating survival in continuous space from mark-dead-recovery data—Towards a continuous version of the multinomial dead recovery model. *Journal of Theoretical Biology*, *574*, 111625. https://doi.org/10.1016/j.jtbi.2023.111625

Seber, G. A. F. (1965). A note on the multiple-recapture census. *Biometrika*, *52*(1/2), 249–259. https://doi.org/10.2307/2333827

Sillett, T. S., & Holmes, R. T. (2002). Variation in survivorship of a migratory songbird throughout its annual cycle. *Journal of Animal Ecology*, *71*(2), 296–308. https://doi.org/10.1046/j.1365-2656.2002.00599.x

Su, Y.-S., & Yajima, M. (2020). *R2jags: Using R to run 'JAGS'* [R package version 0.6-1]. https://CRAN.R-project.org/package=R2jags

Taylor, C. M., & Stutchbury, B. J. M. (2016). Effects of breeding versus winter habitat loss and fragmentation on the population dynamics of a migratory songbird. *Ecological Applications*, *26*(2), 424–437. https://doi.org/10.1890/14-1410

Viana, D. S., Santoro, S., Soriguer, R. C., & Figuerola, J. (2023). A synthesis of Eurasian curlew (*Numenius arquata arquata*) demography and population viability to inform its management. *Ibis*, *165*(3), 767–780. https://doi.org/10.1111/ibi.13184

Von Rönn, J. A. C., Grüebler, M. U., Fransson, T., Köppen, U., & Korner-Nievergelt, F. (2020). Integrating stable isotopes, parasite, and ring-reencounter data to quantify migratory connectivity—A case study with barn swallows breeding in Switzerland, Germany, Sweden, and Finland. *Ecology and Evolution*, *10*(4), 2225–2237. https://doi.org/10.1002/ece3.6061

Webster, M. S., Marra, P. P., Haig, S. M., Bensch, S., & Holmes, R. T. (2002). Links between worlds: Unraveling migratory connectivity. *Trends in Ecology & Evolution*, *17*(2), 76–83. https://doi.org/10.1016/S0169-5347(01)02380-1

Wernham, S. R., Toms, C. V., Marchant, M. P., Clark, J. H., Siriwardena, J. A., & Baillie, G. M. (2002). *Migration atlas: Movements of the birds of Britain and Ireland*. T&AD Poy.

Wilson, S., LaDeau, S. L., Tøttrup, A. P., & Marra, P. P. (2011). Range-wide effects of breeding- and nonbreeding-season climate on the abundance of a Neotropical migrant songbird. *Ecology*, *92*(9), 1789–1798. https://doi.org/10.1890/10-1757.1

Zipkin, E. F., Inouye, B. D., & Beissinger, S. R. (2019). Innovations in data integration for modeling populations. *Ecology*, *100*, e02713. https://doi.org/10.1002/ecy.2713

Zipkin, E. F., Zylstra, E. R., Wright, A. D., Saunders, S. P., Finley, A. O., Dietze, M. C., Itter, M. S., & Tingley, M. W. (2021). Addressing data integration challenges to link ecological processes across scales. *Frontiers in Ecology and the Environment*, *19*(1), 30–38. https://doi.org/10.1002/fee.2290

SUPPORTING INFORMATION

Additional supporting information can be found online in the Supporting Information section at the end of this article.

Appendix S1: Migratory connectivity and demographic data simulation.

Appendix S2: Model adjustment for the Eurasian Curlew.

Appendix S3: Simulations—accuracy and precision of all parameters.

Appendix S4: Eurasian Curlew—estimation of complementary parameters.

How to cite this article: Gregory, K. A., Francesiaz, C., Jiguet, F., Crochet, P.-A., Bocher, P., Düttmann, H., Elts, J., Fartmann, T., Garthe, S., Kämpfer, S., Kruckenberg, H., Marja, R., Piha, M., Schwemmer, P., & Besnard, A. (2025). An integrative framework to combine migratory connectivity and demographic data. *Methods in Ecology and Evolution*, *16*, 596–610. https://doi.org/10.1111/2041-210X.14489